Aerospace Science and Technology 66 (2017) 304–314

Contents lists available at ScienceDirect

Aerospace Science and Technology

www.elsevier.com/locate/aescte

Stochastic analysis of fuel consumption in aircraft cruise subject to along-track wind uncertainty

Rafael Vazquez, Damián Rivas *, Antonio Franco

Department of Aerospace Engineering, Escuela Técnica Superior de Ingeniería, 41092 Sevilla, Spain

ARTICLE INFO

Article history:
Received 20 October 2016
Received in revised form 6 March 2017
Accepted 17 March 2017
Available online 22 March 2017

Keywords:
Stochastic trajectory prediction
Fuel consumption uncertainty
Wind uncertainty
Probability Transformation Method

ABSTRACT

The effects of along-track wind uncertainty on aircraft fuel consumption are analyzed. The case of cruise flight subject to an average constant wind is considered. The average wind is modeled as a random variable, which in this paper is assumed to follow either a uniform or a beta distribution. The probability density function (pdf) of the fuel consumption is obtained using a numerical approach that is based on the Probability Transformation Method (a method that evolves the wind pdf). The dynamics of aircraft mass evolution in cruise flight is defined by a simple nonlinear equation that can be solved analytically; this exact solution is used to assess the accuracy of the method. A general analysis is performed for arbitrary along-track winds. Comparison of the numerical results with the exact analytical solution shows an excellent agreement in all cases. A linear approximation is analyzed as well, which turns out to be very accurate for this problem. The results show that the standard deviation of the fuel mass distribution varies almost linearly with the standard deviation of the wind, whereas the mean of the fuel mass is practically independent of the wind uncertainty. They also show that, for the same along-track wind uncertainty, the uncertainty in the fuel consumption is larger in the case of headwinds than in the case of tailwinds.

1. Introduction

The future Air Traffic Management (ATM) system must address the performance challenges posed by today's airspace: the capacity and the efficiency of the system must be increased while preserving or augmenting the safety levels. To accomplish these goals it is required a paradigm shift in operations through innovative technology and research. In this future system the trajectory becomes the fundamental element of a new set of operating procedures, collectively referred to as Trajectory-Based Operations (TBO), which aim at establishing a trajectory-based ATM system designed to accommodate airspace users' requests to the maximum extent possible [1].

One key factor that affects those challenges is uncertainty, which is an inherent property of real-world socio-technical complex systems, and ATM is clearly not an exception. Uncertainty is critical from different perspectives in air transport: safety, environmental and cost dimensions. Researchers must accept the fact that uncertainty is unavoidable and must be dealt with, rather than ignored. If the capacity of the ATM system is to be increased while maintaining high safety standards and improving the overall performance, uncertainty levels must be reduced and new strategies to deal with the remaining uncertainty must be found. In particular, procedures to integrate uncertainty information into the ATM planning process must be developed. In Rivas and Vazquez [2] one can find a review of all the uncertainty sources that affect the ATM system. Among those, weather has perhaps the greatest impact. Its importance has been extensively assessed in the literature; thus, according to Zelinski and Jastrzebski [3] convective weather is identified as one of the ATM uncertainty factors that most seriously affect the network route structure, and thus the optimal flight trajectory planning.

The analysis of weather uncertainty has been addressed by many authors, using different methods. For instance, Nilim et al. [4] consider a trajectory-based air traffic management scenario to minimize delays under weather uncertainty, where the weather processes are modeled as stationary Markov chains. Pepper et al. [5] present a method, based on Bayesian decision networks, for taking into account uncertain weather information in air traffic flow management. Clarke et al. [6] develop a methodology to study airspace capacity in the presence of weather uncertainty and formulates a stochastic dynamic programming algorithm for traffic flow management. Kim et al. [7] consider different sources of uncertainty (wind and severe weather among them) and derive

* Corresponding author.
E-mail address: drivas@us.es (D. Rivas).

http://dx.doi.org/10.1016/j.ast.2017.03.027
1270-9638/

Nomenclature

A, B	constants of the problem in the aircraft mass equation
C_D, C_L	drag and lift coefficients
C_{D_0}, C_{D_2}	coefficients of the drag polar
c	specific fuel consumption
D	aerodynamic drag
E[.]	expectation
f_y	probability density function of random variable y
g	gravity acceleration
g_A, g_F	wind–mass and wind–fuel transformations
h	altitude
L	lift
m, m_f	aircraft mass and final aircraft mass
m_F	fuel load
n	number of points for the PTM numerical approach
S	wing surface area
T	thrust
t	time
V	aircraft true airspeed
w	average along-track wind speed
$\bar{w}, w_M, w_m$	mean, maximum and minimum values of the average wind distribution
x	horizontal distance
x_f	range
α, β	coefficients of the beta distribution
δ_w	half-width of the wind distribution
ρ	air density
σ[.]	standard deviation
ϕ	sensitivity function of the aircraft mass with respect to the wind speed

service time distributions for different flight phases, assessing traffic flow efficiency by means of queuing network models. Zheng and Zhao [8] develop a statistical model of wind uncertainties and apply it to stochastic trajectory prediction in the case of straight, level flight trajectories. The importance of weather uncertainty information in probabilistic air traffic flow management is shown in Steiner et al. [10], where the translation of ensemble weather forecasts into probabilistic air traffic capacity impact is described. An analysis of wind-optimal cruise trajectories using ensemble probabilistic forecasts and a robust optimal control methodology is performed in Gonzalez-Arribas et al. [9].

In this paper a probabilistic analysis of aircraft fuel consumption taking into account wind uncertainty is presented. Several methods have been proposed to study uncertainty propagation in dynamical systems. The easiest, but more expensive in computational terms, is the classical Monte-Carlo method. Halder and Bhattacharya [11] classify those methods in two categories: parametric (in which one evolves the statistical moments) and non-parametric (in which the probability density function is evolved). In this work, a non-parametric method is applied, in which the wind probability density function (pdf) is evolved. The method used for the uncertainty propagation is based on the Probabilistic Transformation Method (see Kadry [12] and Kadry and Smaily [13]). This method was presented in Vazquez and Rivas [14] where the propagation of uncertainty in the initial aircraft mass was studied, and some preliminary results applied to wind uncertainty are described in Vazquez and Rivas [15]. The approach is based on the resolution of the variational equation for the sensitivity function with respect to the wind.

In this paper a general analysis is performed focusing the study on the cruise phase. This study is relevant because wind is one of the main sources of uncertainty in trajectory prediction, and because cruise uncertainties have a large impact on the overall flight since the cruise phase is the largest portion of the flight (at least for long-haul routes). In particular it is expected that this study be relevant for the determination of the contingency fuel, and, hence, for allowing a more effective decision making, as concluded by SESAR WP-E IMET project (http://www.sesarju.eu/print/2352). In this respect, Hao et al. [16] analyze the cost of carrying the additional discretionary fuel excessively loaded, above a reasonable and conservative buffer, to face flight unpredictability; and Ryerson et al. [17] stress the possibility of achieving substantial savings through the use of a reformed policy for discretionary fuel loading.

The evolution of the aircraft mass in cruise flight is described by a simple nonlinear equation that can be solved analytically. Hence, this exact solution represents a benchmark that is used to assess the performance of the proposed numerical method. The comparison shows an excellent agreement. Moreover, a linear approximation is also made, which is shown to be very accurate for the problem considered in this paper (being within 2% of the exact solution).

In this work, results are presented for arbitrary winds that follow continuous uniform and beta distributions (both symmetric and non-symmetric beta distributions). The uncertainty of the aircraft mass is analyzed first, and its evolution along the trajectory is described. Then, the effects of wind uncertainty on fuel consumption are studied. The results show that the uncertainty in the fuel consumption is larger in the case of headwinds than in the case of tailwinds, for the same value of the wind uncertainty. With respect to the fuel mass distribution, it is shown that the mean is practically independent of the wind uncertainty, whereas its standard deviation does depend on the wind uncertainty, dependence that is roughly linear (for the range of wind uncertainty considered in the paper). These trends are hinted by the results given by the linear approximation.

The outline of the paper is as follows: first, the problem of cruise fuel consumption subject to uncertain winds is formulated (Section 2); in Section 3 the probabilistic wind models are described; in Section 4 an analysis of aircraft mass uncertainty is presented, which is followed by an analysis of fuel consumption uncertainty in Section 5; the linear approximation is presented in Section 6; the results are discussed in Section 7; and finally some conclusions are drawn in Section 8.

2. Cruise trajectory subject to uncertain along-track winds

As already indicated, in this paper the fuel consumption in cruise flight is studied. The cruise is supposed to be formed by a given number of cruise segments, each one of them defined by a constant heading, and flown at constant speed and constant altitude, as required by Air Traffic Control (ATC) procedures. In each cruise segment the flight is assumed to be subject to a constant average wind, which can be different for the different segments, thus modeling the along-track wind variation; the average wind in each segment is modeled as a random variable.

In this paper, as a first step in this research, the case of a cruise defined by only one segment is considered. The case of several cruise segments is left for future work since it involves more than one random variable.

To study the evolution of the aircraft mass in cruise flight, the equations of flight mechanics for flight in a vertical plane (constant course) are considered, under the following hypothesis: symmetric flight, flat Earth model, constant altitude, and constant speed.

Moreover the aircraft is supposed to be subject to a constant along-track wind, which can be thought of as the average wind along the cruise flight. The equations of motion are (see Ref. [18])

$$\frac{dx}{dt} = V + w, \quad \frac{dm}{dt} = -cT \qquad T = D, \quad L = mg \tag{1}$$

where x is the horizontal distance, t is the time, V is the aerodynamic speed, w is the average wind speed (considered constant), T, D, L are the thrust, the aerodynamic drag and the lift, m is the aircraft mass, $g = 9.8$ m/s^2 is the acceleration of gravity, and c is the specific fuel consumption (which can be taken as a function of altitude and speed, and it is therefore constant under the given cruise condition).

The drag can be written as $D = \frac{1}{2}\rho V^2 S C_D$, where ρ is the air density, S the wing surface area, and the drag coefficient C_D is modeled by a parabolic polar $C_D = C_{D_0} + C_{D_2} C_L^2$, where C_L is the lift coefficient given by $C_L = \frac{2L}{\rho V^2 S}$, and the coefficients C_{D_0} and C_{D_2} are constant under the given cruise condition.

Using these definitions and Eqs. (1), the following equation is obtained

$$\frac{dm}{dx} = -\frac{A + Bm^2}{V + w} \tag{2}$$

where the constants A and B are defined as

$$A = \frac{c}{2}\rho V^2 S C_{D_0}, \quad B = \frac{2cC_{D_2}g^2}{\rho V^2 S} \tag{3}$$

Note that $A, B > 0$. Equation (2) is a nonlinear equation describing the evolution of the aircraft mass as a function of distance. Even though this model is quite simple, it is adequate to describe the cruise flight of commercial transport aircraft, since they usually fly segments of constant Mach number (M) and constant altitude (h) following Air Traffic Control procedures, and it is assumed that the constant values of the parameters of the aircraft model (C_{D_0}, C_{D_2} and c) correspond to the values of M and h set for the flight.

In this paper, the cruise range x_f and the final aircraft mass m_f are given. Fixing m_f (instead of the initial aircraft mass) is consistent with having a fixed landing weight. It also allows for a fair comparison for different values of the wind, which lead to different fuel loads and therefore to different values of the initial aircraft mass. Hence, Eq. (2) is to be solved *backwards* with the boundary condition

$$m(x_f) = m_f \tag{4}$$

To emphasize the dependence of the mass $m(x)$ on the wind, it is written as $m(x; w)$, even though often it is just denoted as m for the sake of simplicity. Once the aircraft mass is obtained, the cruise fuel consumption follows from

$$m_F(w) = m(0; w) - m_f \tag{5}$$

If the average wind w is uncertain, then the evolution of mass with distance is uncertain as well. In particular, since the aircraft final mass is fixed for a given cruise range, then the required fuel mass is uncertain. Note that, in such a case, the solution of Eqs. (2)–(4) is still valid but in a probabilistic sense, i.e., $m(x; w)$ is a random process. Notice that in the case of several cruise segments m_f would be uncertain after the first segment, and hence one would have a problem with two random variables.

The mass evolution problem given by Eqs. (2)–(4) has an explicit solution that is given in Appendix A, which is used in this paper to validate the numerical results.

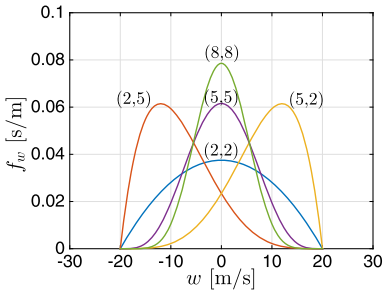

Fig. 1. Wind beta distributions.

3. Probabilistic wind model

In this paper two different distributions are considered for the wind: beta and uniform distributions.

3.1. Beta distribution

The beta distribution is defined by four parameters: the minimum and maximum values of the variable, w_m and w_M, α and β. The probability density function is (see Ref. [19])

$$f_w(w) = \begin{cases} \dfrac{(w - w_m)^{\alpha-1}(w_M - w)^{\beta-1}}{(w_M - w_m)^{\alpha+\beta-1} B(\alpha, \beta)}, & w \in [w_m, w_M] \\ 0, & w \notin [w_m, w_M] \end{cases} \tag{6}$$

where $B(\alpha, \beta)$ is the Euler's beta function, which is obtained in terms of the gamma function as (see Ref. [20])

$$B(\alpha, \beta) = \frac{\Gamma(\alpha)\Gamma(\beta)}{\Gamma(\alpha + \beta)} \tag{7}$$

The mean of w is

$$\bar{w} = \mathrm{E}[w] = \int_{-\infty}^{\infty} w f_w(w) dw = \frac{\alpha w_M + \beta w_m}{\alpha + \beta} \tag{8}$$

where $\mathrm{E}[\cdot]$ is the mathematical expectation, and the standard deviation of w is

$$\sigma[w] = \left[\int_{-\infty}^{\infty} w^2 f_w(w) dw - (\mathrm{E}[w])^2 \right]^{1/2} = \frac{w_M - w_m}{\alpha + \beta} \sqrt{\frac{\alpha\beta}{1 + \alpha + \beta}} \tag{9}$$

In Fig. 1 the pdf is represented for the following cases: $w_m = -20$ m/s and $w_M = +20$ m/s, $(\alpha, \beta) = (2, 2), (5, 5), (8, 8), (2, 5), (5, 2)$. For $\alpha = \beta$ one has symmetric distributions; as α increases, the dispersion of the distribution decreases, as dictated by Eq. (9). On the other hand, for $\alpha \neq \beta$ the pdfs are non-symmetric; for $\alpha > \beta$ the pdf leans to the right, and for $\alpha < \beta$ the pdf leans to the left.

A useful parameter of the distribution, used below, is the half width

$$\delta_w = \frac{1}{2}(w_M - w_m) \tag{10}$$

3.2. Uniform distribution

For the particular case $\alpha = \beta = 1$, the beta distribution reduces to the uniform distribution. The probability density function is now

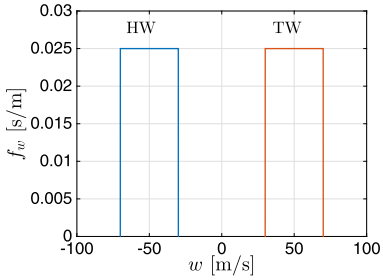

Fig. 2. Wind uniform distributions.

$$f_w(w) = \begin{cases} \dfrac{1}{w_M - w_m}, & w \in [w_m, w_M] \\ 0, & w \notin [w_m, w_M] \end{cases} \tag{11}$$

The mean and the standard deviation of w are now

$$\bar{w} = \frac{w_M + w_m}{2} \tag{12}$$

$$\sigma[w] = \frac{w_M - w_m}{2\sqrt{3}} \tag{13}$$

In Fig. 2 the pdf is represented for the following winds: headwind (HW) $w_m = -70$ m/s, $w_M = -30$ m/s, and tailwind (TW) $w_m = 30$ m/s, $w_M = 70$ m/s. The mean values are HW $\bar{w} = -50$ m/s and TW $\bar{w} = 50$ m/s; and $\delta_w = 20$ m/s in both cases.

4. Analysis of aircraft mass uncertainty

In the following, the aircraft mass is analyzed for a given probabilistic wind model. The objective is to obtain the probability density function of the aircraft mass at a given distance x_A, namely $f_m(m; x_A)$.

In this analysis the Probability Transformation Method (PTM) is considered, which is based on the following theorem (see Canavos [21]): Given a random variable y with probability density function $f_y(y)$, if one defines another random variable z using a transformation g such that $z = g(y)$, then it is known that the probability density function of z is given by

$$f_z(z) = \frac{f_y(g^{-1}(z))}{|g'(g^{-1}(z))|} \tag{14}$$

an expression that is valid only if the function $g(y)$ is invertible on the domain of y.

In this problem,

$$f_m(m; x_A) = \frac{f_w(g_A^{-1}(m))}{|g'_A(g_A^{-1}(m))|} \tag{15}$$

where the transformation $m = g_A(w)$ is defined by

$$g_A(w) = m(x_A; w) \tag{16}$$

(note that g_A depends on the given value of x_A). Thus, the analysis is valid only if the function $g_A(w)$ is invertible on the domain of w, that is, only if for two different values of wind w_1 and w_2, the aircraft masses m_1 and m_2 are different, which in this problem is obvious.

In this paper the numerical method developed in Vazquez and Rivas [14] to compute Eq. (14) is used, which is summarized next for completeness. The first step consists in taking n consecutive points from the domain of w, denoted as w^i, $i = 1, \ldots, n$, so that $w^1 < w^2 < \ldots < w^n$. Now, solving backwards the mass equation (Eq. (2)) for each i with parameter w^i and m_f as final condition, one can compute the value of the aircraft mass at $x = x_A$, $m^i(x_A) = m(x_A; w^i)$. The numerator of Eq. (15) is computed for each i as $f_w(w^i)$. To compute the denominator of Eq. (15), the function $g'_A(w)$ is needed; this function is obtained in terms of

$$\phi(x; w) \equiv \frac{\partial m(x; w)}{\partial w} \tag{17}$$

which is the sensitivity function of the solution m with respect to the parameter w. That is, from Eq. (16) one has

$$g'_A(w) = \frac{\partial m(x_A; w)}{\partial w} = \phi(x_A; w) \tag{18}$$

The process to obtain $\phi(x; w)$ is presented in Appendix B. Once the function $\phi(x_A; w)$ is found, the denominator of Eq. (15) is computed for each i as $|g'_A(w^i)| = |\phi(x_A; w^i)|$. Hence, one has the values of the probability density function $f_m(m; x_A)$ at the n points m^i, $i = 1, \ldots, n$, as

$$f_m(m^i; x_A) = \frac{f_w(w^i)}{|\phi(x_A; w^i)|} \tag{19}$$

Notice that the computation of the denominator of Eq. (15) is independent of the probabilistic model considered for the wind.

Once the discretized pdf is obtained, one can compute numerically the mean and the standard deviation, which are defined as follows

$$E[m(x_A; w)] = \int_{-\infty}^{\infty} m f_m(m; x_A) dm \tag{20}$$

$$\sigma[m(x_A; w)] = \left[\int_{-\infty}^{\infty} m^2 f_m(m; x_A) dm - (E[m(x_A; w)])^2 \right]^{1/2} \tag{21}$$

5. Analysis of fuel consumption uncertainty

In this section the previous results are applied to analyze the fuel consumption uncertainty. The application is straightforward based on the definition (Eq. (5))

$$m_F(w) = m(0; w) - m_f$$

The analysis of the fuel mass pdf reduces to the analysis of the aircraft mass pdf (Section 4) for $x_A = 0$. If one defines the transformation $m_F = g_F(w)$ by

$$g_F(w) = m(0; w) - m_f \tag{22}$$

then one has

$$f_{m_F}(m_F) = \frac{f_w(g_F^{-1}(m_F))}{|g'_F(g_F^{-1}(m_F))|} \tag{23}$$

For each value of the wind w^i, $i = 1, \ldots, n$, one has

$$m_F^i = m(0; w^i) - m_f \tag{24}$$

Also,

$$g'_F(w) = \frac{\partial m(0; w)}{\partial w} = \phi(0; w) \tag{25}$$

therefore, for each i one has $|g'_F(w^i)| = |\phi(0; w^i)|$ and, hence,

$$f_{m_F}(m_F^i) = \frac{f_w(w^i)}{|\phi(0; w^i)|} \tag{26}$$

As before, once the discretized pdf is obtained, one can compute numerically the mean and the standard deviation, defined as follows

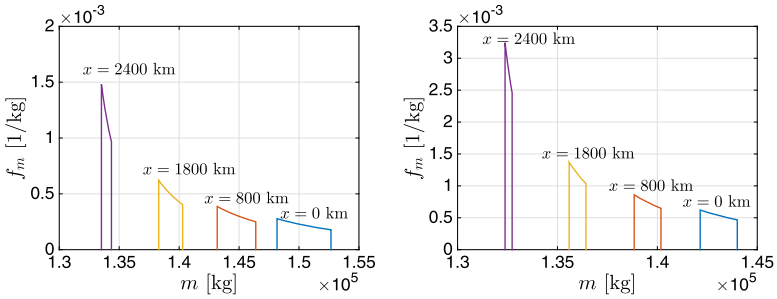

Fig. 3. Aircraft mass pdf at $x = 0, 800, 1800, 2400$ km. a) HW $\bar{w} = -50$ m/s, b) TW $\bar{w} = 50$ m/s; $\delta_w = 20$ m/s. Uniform wind distribution.

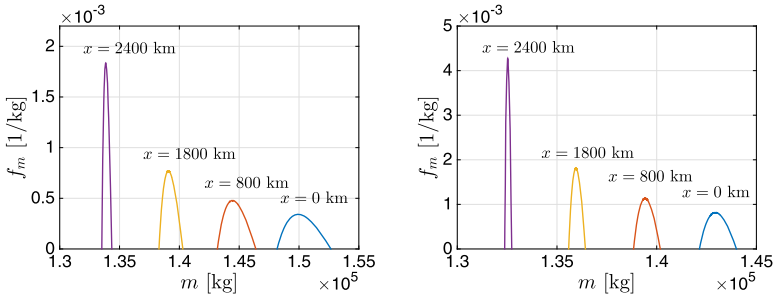

Fig. 4. Aircraft mass pdf at $x = 0, 800, 1600, 2400$ km. a) HW $\bar{w} = -50$ m/s, b) TW $\bar{w} = 50$ m/s; $\delta_w = 20$ m/s. Beta-symmetric wind distribution ($\alpha = \beta = 2$).

$$E[m_F(w)] = \int_{-\infty}^{\infty} m_F f_{m_F}(m_F) dm_F \tag{27}$$

$$\sigma[m_F(w)] = \left[\int_{-\infty}^{\infty} m_F^2 f_{m_F}(m_F) dm_F - (E[m_F(w)])^2 \right]^{1/2} \tag{28}$$

6. Linear approximation

In some applications, the pdf is not required and only the mean and the standard deviation are needed. Then, as an alternative to PTM, one can simply substitute the function $z = g(y)$ by its linear approximation: $z \approx g(y_0) + g'(y_0)(y - y_0)$. If the point y_0 is taken as the mean value of y, this is, $y_0 = E[y]$, then $z \approx g(E[y]) + g'(E[y])(y - E[y])$. One then finds (see [22] for details)

$$E[z] \approx g(E[y]) \tag{29}$$

$$\sigma[z] \approx \sigma[y] \left| g'(E[y]) \right| \tag{30}$$

The quality of the approximation obviously depends on the non-linearity of the function g.

Applying this approximation to the analysis of the fuel consumption uncertainty, one obtains

$$E[m_F(w)] \approx g_F(\bar{w}), \tag{31}$$

$$\sigma[m_F(w)] \approx \sigma[w] \left| g_F'(\bar{w}) \right| \tag{32}$$

Particular results will be shown in Section 7.3, comparing the mean and the standard deviation obtained by using the PTM and the linear approximation.

7. Results

Results are presented for a given aircraft and a given cruise flight defined by the following values of the different parameters: $V = 240$ m/s, $\rho = 0.4127$ kg/m^3 ($h \approx 10000$ m), $C_{D_0} = 0.01744$, $C_{D_2} = 0.04823$, $c = 1.49 \cdot 10^{-5}$ s/m, $S = 283.5$ m^2, $m_f = 130000$ kg, and $x_f = 3000$ km. The aircraft model data correspond to a Boeing 767-400, as provided by Eurocontrol's BADA data base [23]. In the numerical computations, for the PTM the number of points taken is $n = 1000$, value that has proven to be good enough.

Three different wind distributions are analyzed: uniform ($\alpha = \beta = 1$), beta symmetric $\alpha = \beta = 2$ and beta non-symmetric $\alpha = 2, \beta = 8$. For each type of distribution, different cases are considered. Instead of varying the minimum and maximum values, w_m and w_M, the values of the mean and the half-width, $\bar{w}$ and δ_w, are varied (which is an equivalent way of defining the distribution). Results are presented for $\bar{w}$ ranging between -50 m/s and 50 m/s, and δ_w ranging between 0 and 30 m/s. Note that the standard deviation, which is given by

$$\sigma[w] = \frac{2\delta_w}{\alpha + \beta} \sqrt{\frac{\alpha\beta}{1 + \alpha + \beta}} \tag{33}$$

is different for the three wind distributions; for example, for $\delta_w = 20$ m/s one has: $\sigma[w] = 11.55$ m/s for the uniform distribution, $\sigma[w] = 8.94$ m/s for the beta symmetric and $\sigma[w] = 4.82$ m/s for the beta non-symmetric.

7.1. Aircraft mass distribution

In this section the evolution of the aircraft mass uncertainty is analyzed. The pdfs of the aircraft mass at several distances ($x = 0, 800, 1800, 2400$ km) are represented in Figs. 3, 4 and 5 for the three wind distributions (uniform, beta symmetric and beta non-symmetric, respectively), for $\bar{w} = -50, 50$ m/s and $\delta_w = 20$ m/s.

It can be seen that the width of the mass distribution decreases as the flown distance increases, that is, the uncertainty in the aircraft mass decreases along the cruise, being largest at $x = 0$. Since one has $m(0; w) = m_F(w) + m_f$, one can see that this initial uncertainty is precisely the uncertainty in the fuel mass, which is

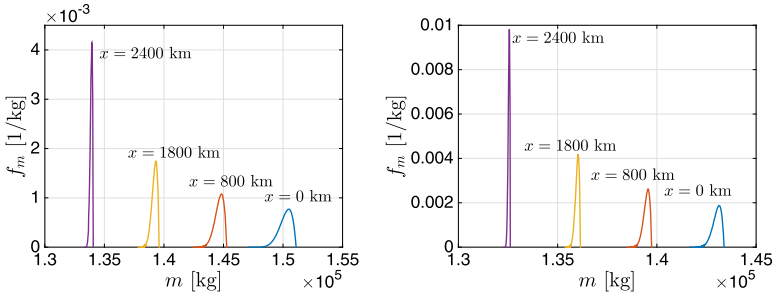

Fig. 5. Aircraft mass pdf at $x = 0, 800, 1600, 2400$ km. a) HW $\bar{w} = -50$ m/s, b) TW $\bar{w} = 50$ m/s; $\delta_w = 20$ m/s. Beta-nonsymmetric wind distribution ($\alpha = 2$, $\beta = 8$).

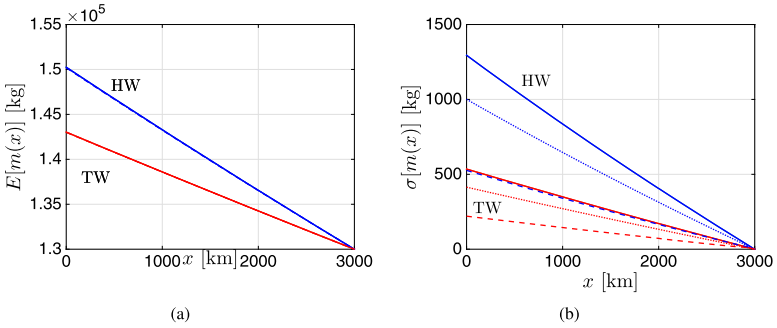

Fig. 6. Mean and standard deviation of aircraft mass as function of flown distance. HW $\bar{w} = -50$ m/s and TW $\bar{w} = 50$ m/s; $\delta_w = 20$ m/s. Uniform wind distribution ($\alpha = 1, \beta = 1$), solid; beta-symmetric ($\alpha = 2, \beta = 2$), dotted; and beta-nonsymmetric ($\alpha = 2, \beta = 8$) dashed.

Table 1
Mean and standard deviation of the initial aircraft mass for the different wind distributions ($\bar{w} = -50, 50$ m/s; $\delta_w = 20$ m/s).

Wind	E[$m(0)$] (kg)		$\sigma[m(0)]$ (kg)	
	HW	TW	HW	TW
$\alpha = 1, \beta = 1$	150251.4	143027.4	1295.0	535.2
$\alpha = 2, \beta = 2$	150218.3	143018.6	1000.8	414.2
$\alpha = 2, \beta = 8$	150183.0	143009.2	525.9	219.9

analyzed in the next subsection. The mean and the standard deviation of the aircraft mass as a function of flown distance are represented in Fig. 6. Note that at $x = x_f$ one has $E[m] = m_f$ and $\sigma[m] = 0$, as it corresponds to the final boundary condition. Some numerical values for $x = 0$ are collected in Table 1.

Note that the larger the wind uncertainty the larger the aircraft mass uncertainty. In fact, for the three distributions considered, one has

$$\sigma[w]_u > \sigma[w]_{b\text{-}s} > \sigma[w]_{b\text{-}ns}$$
$$\Rightarrow \sigma[m(0)]_u > \sigma[m(0)]_{b\text{-}s} > \sigma[m(0)]_{b\text{-}ns} \quad (34)$$

where *u*, *b-s* and *b-ns* stand for uniform, beta symmetric and beta non-symmetric, respectively. However, in Section 7.3 it is shown that $\sigma[m(0)]/\sigma[w]$ is practically independent of the wind distribution, provided that the same value of $\bar{w}$ is taken.

7.2. Fuel consumption distribution

7.2.1. Uniform wind distribution

First, fuel distributions are represented for the following wind distributions: HW $\bar{w} = -50$ m/s and TW $\bar{w} = 50$ m/s, with $\delta_w = 10, 20, 30$ m/s; the corresponding pdfs are depicted in Fig. 7.

Next, the mean and the standard deviation of the fuel consumption are represented in Fig. 8 and Fig. 9, as a function of the mean wind value $\bar{w}$ for different values of the wind distribution width δ_w ($\delta_w = 5, 10, 15, 20, 25$ m/s), and as a function of δ_w for different values of $\bar{w}$ ($\bar{w} = -50, -40, ...40, 50$ m/s). Some results, for $\bar{w} = -50, 50$ m/s and $\delta_w = 10, 20, 30$ m/s, are given in Table 2.

Table 2
Mean and standard deviation of the fuel consumption. Uniform wind distribution.

$\bar{w}$	E[m_F] (kg)		$\sigma[m_F]$ (kg)	
	-50 m/s	50 m/s	-50 m/s	50 m/s
$\delta_w = 10$ m/s	20189.5	13011.0	643.2	266.8
$\delta_w = 20$ m/s	20251.4	13027.4	1295.0	535.2
$\delta_w = 30$ m/s	20356.1	13055.0	1964.8	806.5

The previous figures show that the mean of the fuel mass distribution decreases as $\bar{w}$ increases (as expected, HWs lead to larger fuel consumption than TWs), and it is practically independent of δ_w. On the other hand, one has that the standard deviation of the fuel mass also decreases as $\bar{w}$ increases, and it increases as δ_w increases. One also has that the fuel uncertainty increases almost linearly with the wind uncertainty (for the range of values of δ_w considered), with a slope that decreases as $\bar{w}$ increases. One obtains the result that the uncertainty in the fuel consumption is larger in the case of HWs (for a given value of the wind uncertainty) than in the case of TWs; as a numerical reference, for $\delta_w = 20$ m/s, $\sigma[m_F]$ increases from 535.2 kg for TW $\bar{w} = 50$ m/s to 1295.0 kg for HW $\bar{w} = -50$ m/s.

7.2.2. Beta-symmetric wind distribution

The pdfs of the wind and the fuel mass are now represented in Fig. 10 for the same values of $\bar{w}$ and δ_w as before; note that although the wind distributions considered are symmetric, the fuel mass pdfs are not. The variation of the mean as a function of $\bar{w}$ and δ_w is very similar to the previous one (Fig. 8); graphically the curves are almost identical, and therefore for brevity are not represented here. The standard deviation is represented in Fig. 11. Some numerical values are given in Table 3.

These results show the same trends as before for E[m_F] and $\sigma[m_F]$. Again, one obtains the result that the uncertainty in the fuel consumption is larger in the case of HWs (for a given value

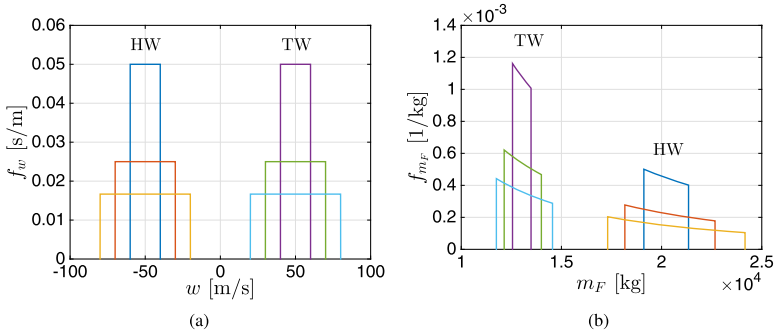

(a) (b)

Fig. 7. a) Uniform wind distributions. b) Fuel consumption distributions. HW $\bar{w} = -50$ m/s, TW $\bar{w} = 50$ m/s; $\delta_w = 10, 20, 30$ m/s.

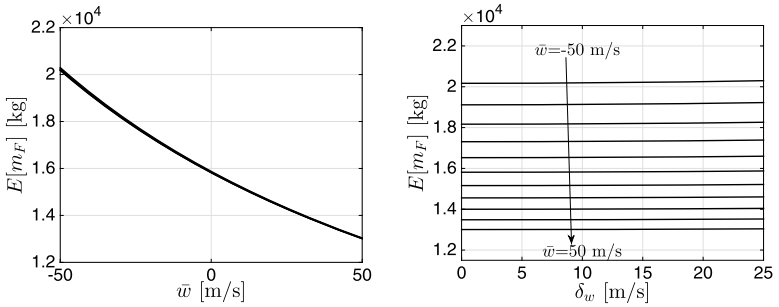

(a) (b)

Fig. 8. Fuel mean a) as a function of $\bar{w}$, $\delta_w = 5, 10, 15, 20, 25$ m/s; b) as a function of δ_w, $\bar{w} = -50, -40, ..., 40, 50$ m/s. Uniform wind distribution.

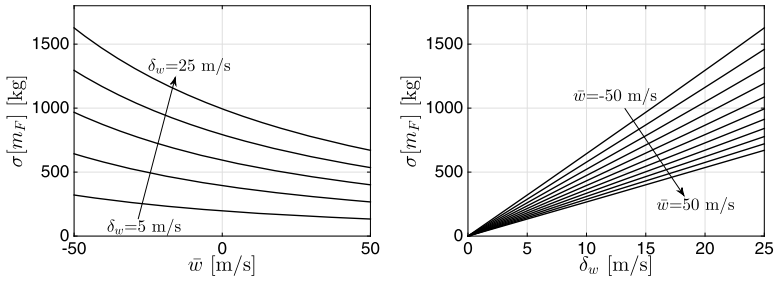

(a) (b)

Fig. 9. Fuel standard deviation a) as a function of $\bar{w}$, $\delta_w = 5, 10, 15, 20, 25$ m/s; b) as a function of δ_w, $\bar{w} = -50, -40, ..., 40, 50$ m/s. Uniform wind distribution.

Table 3
Mean and standard deviation of the fuel consumption. Beta-symmetric wind distribution ($\alpha = 2, \beta = 2$).

$\bar{w}$	E[m_F] (kg)		$\sigma[m_F]$ (kg)	
	−50 m/s	50 m/s	−50 m/s	50 m/s
$\delta_w = 10$ m/s	20181.3	13008.8	497.9	206.7
$\delta_w = 20$ m/s	20218.3	13018.6	1000.8	414.2
$\delta_w = 30$ m/s	20280.7	13035.2	1513.9	623.4

Table 4
Mean and standard deviation of the fuel consumption. Beta-nonsymmetric wind distribution ($\alpha = 2, \beta = 8$).

$\bar{w}$	E[m_F] (kg)		$\sigma[m_F]$ (kg)	
	−50 m/s	50 m/s	−50 m/s	50 m/s
$\delta_w = 10$ m/s	20172.5	13006.4	265.3	110.6
$\delta_w = 20$ m/s	20183.0	13009.2	525.9	219.9
$\delta_w = 30$ m/s	20200.2	13013.9	782.8	327.9

of the wind uncertainty) than in the case of TWs; as a numerical reference, for $\delta_w = 20$ m/s and $\alpha = \beta = 2$, $\sigma[m_F]$ increases from 414.2 kg for TW ($\bar{w} = 50$ m/s) to 1000.8 kg for HW ($\bar{w} = -50$ m/s).

7.2.3. Beta-nonsymmetric wind distribution

The pdfs of the wind and the fuel mass are now represented in Fig. 12 for the same $\bar{w}$ and δ_w as in the previous cases. As before, the variation of the mean, being almost identical to the previous cases, is not represented here for brevity. The standard deviation is represented in Fig. 13. Some numerical values are given in Table 4.

These results show the same trends as before. Once more, one obtains the result that the uncertainty in the fuel consumption is larger in the case of HWs (for a given value of the wind uncertainty) than in the case of TWs.

7.3. Comparison of fuel consumption results

7.3.1. Comparison of different methods

In this section the numerical solution is compared to the exact solution given in Appendix A, and also the solution obtained with the linear method is compared to them. The comparison is made for the fuel consumption. Results for $\bar{w} = -50, 50$ m/s and $\delta_w = 20$ m/s are given in Tables 5, 6 and 7, including the relative errors. The PTM and the exact solution are almost identical.

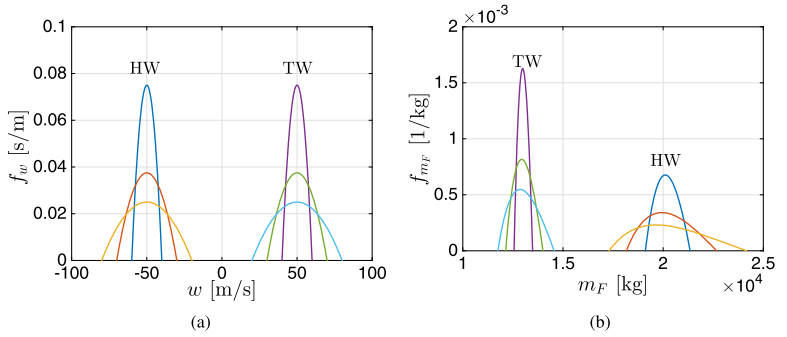

Fig. 10. a) Beta-symmetric wind distributions. b) Fuel consumption distributions. Case $\alpha = 2, \beta = 2$. HW $\bar{w} = -50$ m/s, TW $\bar{w} = 50$ m/s; $\delta_w = 10, 20, 30$ m/s.

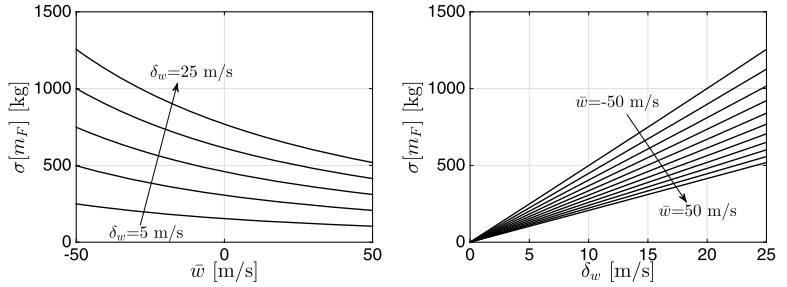

Fig. 11. Fuel standard deviation a) as a function of $\bar{w}$, $\delta_w = 5, 10, 15, 20, 25$ m/s; b) as a function of δ_w, $\bar{w} = -50, -40, ..., 40, 50$ m/s. Beta-symmetric wind distribution ($\alpha = \beta = 2$).

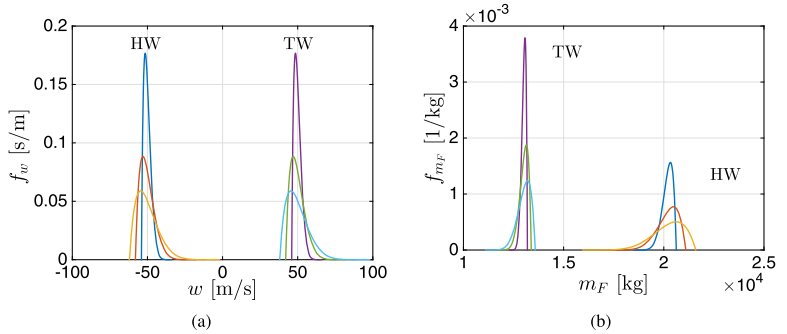

Fig. 12. a) Beta-nonsymmetric wind distributions. b) Fuel consumption distributions. Case $\alpha = 2, \beta = 8$. HW $\bar{w} = -50$ m/s, TW $\bar{w} = 50$ m/s; $\delta_w = 10, 20, 30$ m/s.

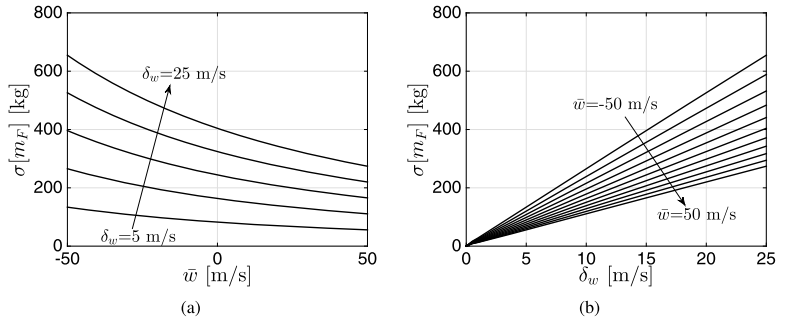

Fig. 13. Fuel standard deviation a) as a function of $\bar{w}$, $\delta_w = 5, 10, 15, 20, 25$ m/s; b) as a function of δ_w, $\bar{w} = -50, -40, ..., 40, 50$ m/s. Beta-nonsymmetric wind distribution ($\alpha = 2$, $\beta = 8$).

Table 5
Mean and standard deviation of the fuel mass distribution. Uniform wind distribution.

Method	E[m_F] (kg)	E[m_F] error (%)	$\sigma[m_F]$ (kg)	$\sigma[m_F]$ error (%)
$\bar{w} = -50$ m/s, $\delta_w = 20$ m/s				
Exact	20251.4		1295.0	
PTM ($n = 1000$)	20251.4	8.2×10^{-7}	1295.0	2.0×10^{-4}
Linearization	20169.0	0.41	1283.4	0.90
$\bar{w} = 50$ m/s, $\delta_w = 20$ m/s				
Exact	13027.4		535.2	
PTM ($n = 1000$)	13027.4	3.4×10^{-7}	535.2	2.0×10^{-4}
Linearization	13005.5	0.17	533.2	0.37

Table 6
Mean and standard deviation of the fuel mass distribution. Beta-symmetric wind distribution ($\alpha = \beta = 2$).

Method	E[m_F] (kg)	E[m_F] error (%)	$\sigma[m_F]$ (kg)	$\sigma[m_F]$ error (%)
$\bar{w} = -50$ m/s, $\delta_w = 20$ m/s				
Exact	20218.3		1000.8	
PTM ($n = 1000$)	20218.3	9.5×10^{-5}	1000.8	2.5×10^{-4}
Linearization	20169.0	0.24	994.2	0.66
$\bar{w} = 50$ m/s, $\delta_w = 20$ m/s				
Exact	13018.6		414.2	
PTM ($n = 1000$)	13018.6	9.7×10^{-5}	414.2	2.5×10^{-4}
Linearization	13005.5	0.10	413.0	0.27

Table 7
Mean and standard deviation of the fuel mass distribution. Beta-nonsymmetric wind distribution ($\alpha = 2$, $\beta = 8$).

Method	E[m_F] (kg)	E[m_F] error (%)	$\sigma[m_F]$ (kg)	$\sigma[m_F]$ error (%)
$\bar{w} = -50$ m/s, $\delta_w = 20$ m/s				
Exact	20183.0		525.9	
PTM ($n = 1000$)	20182.9	6.2×10^{-4}	525.9	9.0×10^{-4}
Linearization	20169.0	0.07	536.2	1.95
$\bar{w} = 50$ m/s, $\delta_w = 20$ m/s				
Exact	13009.2		219.9	
PTM ($n = 1000$)	13009.2	6.1×10^{-4}	219.9	8.6×10^{-4}
Linearization	13005.5	0.03	222.8	1.31

The linear approach gives a good approximation, within 2% of the exact solution in all cases considered.

7.3.2. Influence of wind distributions

In this paper three wind distributions have been considered (recall that for a given value of $\bar{w}$ the three distributions have different standard deviations). The influence of the wind distribution on the mean of the fuel mass is very small. For HWs it varies between 20183.0 kg and 20251.4 kg (see Tables 5–7), that is, a variation of just 0.34%. For TWs it varies between 13009.2 kg and 13027.4 kg, with a variation of just 0.14%. This result can be easily understood with the help of the linear approximation (Eq. (31)), which states that, to first order approximation, the mean of the fuel mass is independent of the wind uncertainty. The value given by the linear approximation is $E[m_F(w)] = g_F(\bar{w})$, which equals 20169.0 kg for HW $\bar{w} = -50$ m/s and 13005.5 kg for TW $\bar{w} = 50$ m/s). Therefore, for a given value of $\bar{w}$, the influence of the type of distribution on $E[m_F]$ is very small.

On the contrary, for a given value of $\bar{w}$, the standard deviation of the fuel consumption does depend on the wind distribution, because it depends on the wind standard deviation. For HWs it varies between 525.9 kg and 1295.0 kg (see Tables 5–7), and for TWs between 291.9 kg and 535.2 kg. Again, the linear approximation (Eq. (32)) helps in understanding this result: to first order approximation the standard deviation of the fuel mass varies linearly with the standard deviation of the wind distribution. The result given by the linear approximation is

$$\sigma[m_F(w)] = \sigma[w] \left| g'_F(\bar{w}) \right| \tag{35}$$

where $\left| g'_F(\bar{w}) \right|$ equals 111.15 kg/m for HW $\bar{w} = -50$ m/s, $\delta_w = 20$ m/s, and 46.18 kg/m for TW $\bar{w} = 50$ m/s, $\delta_w = 20$ m/s.

Finally, one can also conclude that the quotient $\sigma[m_F]/\sigma[w]$ is practically independent of the wind uncertainty; but it depends strongly on the mean of the wind distribution, being larger for HWs than for TWs. Note that for the linear approximation (Eq. (35)) the quotient is given by $\left| g'_F(\bar{w}) \right|$, depending only on $\bar{w}$. This quotient is represented in Fig. 14 for the three distributions considered in the paper, for $\delta_w = 10, 20, 30$ m/s, and also for the linear approximation. This final figure summarizes the analysis performed in the paper, and provides a quantitative measure of the fuel consumption uncertainty as a function of the stochastic wind that is affecting the flight.

8. Conclusions

The general framework for this paper is the development of a methodology to manage weather uncertainty suitable to be integrated into the trajectory planning process. This work is a first step focused on the assessment of the impact of wind uncertainty on aircraft trajectory, and in particular on cruise fuel load. It is expected that by considering the weather uncertainty in the trajectory prediction process, one could adjust the contingency fuel depending on the uncertainty obtained for the fuel consumption.

The problem of fuel consumption in cruise flight subject to an uncertain along-track average wind has been studied, using a

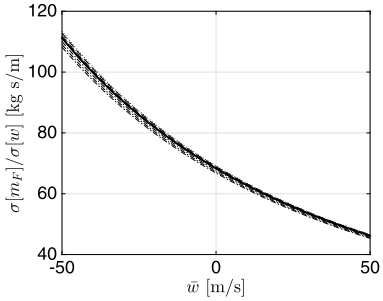

Fig. 14. Quotient $\sigma[m_F]/\sigma[w]$ as a function of $\bar{w}$, for $(\alpha, \beta) = (1, 1), (2, 2), (2, 8)$ with $\delta_w = 10, 20, 30$ m/s and for the linear approximation (thick line).

nonlinear model that has known analytical solution. The average wind has been modeled as a random variable with uniform and beta distribution functions. The analysis has been performed using an approximate numerical method developed by the authors. This method is applicable to problems in which there is just one random variable and for the analysis of functions of the random variable which are invertible. One should note that the numerical approach developed does not require to know the solution of the equations of motion, and also that it is very versatile, valid for any wind distribution taken as input. On the other hand, the Probability Transformation Method on which it is based provides not only the mean and the standard deviation, but the complete pdf of the stochastic solution, as opposed to other methods (such as Polynomial Chaos) which do not provide the pdf.

The results obtained with this numerical method have been compared with the exact analytical results, showing an excellent agreement in all cases; thus, the accuracy of the method has been assessed. The accuracy of a simple linear approach has been also assessed: the linear approximation turns out to be very accurate for the problem studied in this paper. The results have shown that, for given wind uncertainty, the uncertainty in fuel consumption is larger for headwinds than for tailwinds; this result also holds if one considers a relative measure of the uncertainty, for example the metric $\sigma[m_F]/E[m_F]$. The results also show that, for given $\bar{w}$, the standard deviation of the fuel consumption varies almost linearly with the standard deviation of the wind. A quantitative measure of these trends has been provided.

Even though the analysis presented has not taken crosswinds into account, they can be considered in a simple manner by defining the ground speed as $V_g = \sqrt{V^2 - w_c^2} + w$, where w_c is the average crosswind. The analysis now can be carried out straightforwardly just considering V_g as the random variable (instead of w).

The application of the probabilistic approach presented in this paper to trajectories composed of several cruise segments, and taking into account the wind distributions obtained from real weather forecasts, is to be carried out as a next step in this research. Also for future work is left the application to other flight phases defined by more complicated flight conditions, and to other uncertainty sources such as the air temperature uncertainty.

Conflict of interest statement

The authors declare that they have no conflicts of interest associated with this work.

Acknowledgements

The authors gratefully acknowledge the financial support of the Spanish Ministerio de Economía y Competitividad through grant TRA2014-58413-C2-1-R, co-financed with FEDER funds.

Appendix A. Exact solution

The explicit solution of Eqs. (2) and (4) for the aircraft mass is

$$m(x; w) = \sqrt{\frac{A}{B}} \frac{m_f + \sqrt{\frac{A}{B}} \tan\left(\frac{\sqrt{AB}(x_f - x)}{V + w}\right)}{\sqrt{\frac{A}{B}} - m_f \tan\left(\frac{\sqrt{AB}(x_f - x)}{V + w}\right)} \tag{A.1}$$

and the cruise fuel load is

$$m_F = \frac{\left(m_f^2 + \frac{A}{B}\right) \tan\left(\frac{\sqrt{AB}x_f}{V + w}\right)}{\sqrt{\frac{A}{B}} - m_f \tan\left(\frac{\sqrt{AB}x_f}{V + w}\right)} \equiv g_F(w) \tag{A.2}$$

The fuel mass probability density function is (see Eq. (23))

$$f_{m_F}(m_F) = \begin{cases} f_w(g_F^{-1}(m_F))G(m_F), & m_F \in [m_{F_1}, m_{F_2}] \\ 0, & m_F \notin [m_{F_1}, m_{F_2}] \end{cases} \tag{A.3}$$

where

$$G(m_F) = \frac{Ax_f}{(m_f + m_F)^2 + \frac{A}{B}} \left[\arctan\left(\frac{m_F\sqrt{\frac{A}{B}}}{m_f(m_f + m_F) + \frac{A}{B}}\right)\right]^{-2} \tag{A.4}$$

$$g_F^{-1}(m_F) = \frac{\sqrt{AB}x_f}{\arctan\left[\frac{m_F\sqrt{\frac{A}{B}}}{m_f(m_f + m_F) + \frac{A}{B}}\right]} - V \tag{A.5}$$

$$m_{F_1} = g_F(w_m), \quad m_{F_2} = g_F(w_M) \tag{A.6}$$

Note that the G function depends only on the transformation g_F, being independent of the probabilistic wind model considered.

Appendix B. Mass sensitivity function

The sensitivity function $\phi(x; w)$ is obtained as the solution of the following differential equation

$$\frac{\mathrm{d}}{\mathrm{d}x}\phi(x; w) = \frac{\mathrm{d}}{\mathrm{d}x}\left(\frac{\partial m}{\partial w}\right) = \frac{A + Bm^2}{(V + w)^2} - \frac{2Bm}{V + w}\frac{\partial m}{\partial w}$$
$$= \frac{A + Bm^2}{(V + w)^2} - \frac{2Bm}{V + w}\phi(x; w) \tag{B.1}$$

with final condition

$$\phi(x_f; w) = \frac{\partial m(x_f; w)}{\partial w} = \frac{\partial m_f}{\partial w} = 0 \tag{B.2}$$

where $m = m(x; w)$ is defined by (Eqs. (2) and (4))

$$\frac{\mathrm{d}m}{\mathrm{d}x} = -\frac{A + Bm^2}{V + w}$$
$$m(x_f) = m_f$$

This problem is to be solved numerically backwards from $x = x_f$ to $x = 0$.

References

[1] SESAR Consortium, The ATM target concept – SESAR definition phase, deliverable 3, September 2007.

[2] D. Rivas, R. Vazquez, Uncertainty, in: A. Cook, D. Rivas (Eds.), Complexity Science in Air Traffic Management, Routledge, London, 2016, Chapter 4.

[3] S. Zelinski, M. Jastrzebski, Defining dynamic route structure for airspace configuration, Proc. Inst. Mech. Eng., G J. Aerosp. Eng. 226 (9) (2012) 1161–1170.

[4] A. Nilim, L. El Ghaoui, M. Hansen, V. Duong, Trajectory-based air traffic management (TB-ATM) under weather uncertainty, in: Proc. 5th USA–Europe ATM Seminar, ATM2003, 2003, pp. 1–10.

[5] J.W. Pepper, K.R. Mills, L.A. Wojcik, Predictability and uncertainty in air traffic flow management, in: Proc. 4th USA–Europe ATM Seminar, ATM2001, 2001, pp. 1–11.

[6] J. Clarke, S. Solak, Y. Chang, L. Ren, L. Vela, Air traffic flow management in the presence of uncertainty, in: Proc. 8th USA–Europe ATM Seminar, ATM2009, 2009, pp. 1–10.

[7] J. Kim, M. Tandale, P.K. Menon, Air-traffic uncertainty models for queuing analysis, in: AIAA Aviation Technology, Integration and Operations Conference, ATIO, 2009, pp. 1–23, paper AIAA 2009-7053.

[8] Q.M. Zheng, Y.J. Zhao, Modeling wind uncertainties for stochastic trajectory synthesis, in: AIAA Aviation Technology, Integration and Operations Conference, ATIO, 2011, pp. 1–22, paper AIAA 2011-6858.

[9] D. Gonzalez-Arribas, M. Soler, M. Sanjurjo, Wind-based robust trajectory optimization using meteorological ensemble probabilistic forecasts, in: Proc. 6th SESAR Innovation Days, SID2016, 2016, pp. 1–8.

[10] M. Steiner, R. Bateman, D. Megenhardt, Y. Liu, M. Xu, M. Pocernich, J.A. Krozel, Translation of ensemble weather forecasts into probabilistic air traffic capacity impact, Air Traffic Control Q. 18 (3) (2010) 229–254.

[11] A. Halder, R. Bhattacharya, Dispersion analysis in hypersonic flight during planetary entry using stochastic Liouville equation, J. Guid. Control Dyn. 34 (2) (2011) 459–474.

[12] S. Kadry, On the generalization of probabilistic transformation method, Appl. Math. Comput. 190 (2007) 1284–1289.

[13] S. Kadry, K. Smaily, Using the transformation method to evaluate the probability density function of $z = x^{\alpha} y^{\beta}$, Int. J. Appl. Econ. Finance 4 (3) (2010) 181–188.

[14] R. Vazquez, D. Rivas, Propagation of initial mass uncertainty in aircraft cruise flight, J. Guid. Control Dyn. 36 (2) (2013) 415–429.

[15] R. Vazquez, D. Rivas, Analysis of the effect of uncertain average winds on cruise fuel load, in: Proc. 5th SESAR Innovation Days, SID2015, 2015, pp. 1–7.

[16] L. Hao, M. Hansen, M.S. Ryerson, Fueling for contingencies: the hidden cost of unpredictability in the air transportation system, Transp. Res. D 44 (2016) 199–210.

[17] M.S. Ryerson, M. Hansen, L. Hao, M. Seelhorst, Landing on empty: estimating the benefits from reducing fuel uplift in US Civil Aviation, Environ. Res. Lett. 10 (2015) 1–11, 094002.

[18] N. Vinh, Flight Mechanics of High-Performance Aircraft, Cambridge University Press, New York, 1993, p. 112.

[19] K. Bury, Statistical Distributions in Engineering, Cambridge University Press, New York, 1999, pp. 243–244.

[20] M. Abramowitz, I.A. Stegun, Handbook of Mathematical Functions, 9th edition, Dover, 1965, p. 258.

[21] G. Canavos, Applied Probability and Statistical Methods, Little, Brown, Boston, 1984, p. 142.

[22] J.A. Rice, Mathematical Statistics and Data Analysis, Thomson Brooks/Cole, Belmont, California, 2007, p. 162.

[23] A. Nuic, User Manual for the Base of Aircraft Data (BADA), revision 3.13, Eurocontrol, 2015, p. 1.